

Solid state NMR measurements of conformation and conformational distributions in the membrane-bound HIV-1 fusion peptide

Jun Yang, Paul D. Parkanzky, Bhagyashree A. Khunte, Christian G. Canlas, Rong Yang, Charles M. Gabrys, and David P. Weliky

Department of Chemistry, Michigan State University, East Lansing, MI, USA

The solid state NMR lineshape of a protein backbone carbonyl nucleus is a general diagnostic of the local conformational distribution in the vicinity of that nucleus. In addition, measurements of carbonyl chemical shifts and 2D exchange spectra provide information about the most probable conformation in the distribution. These types of solid state NMR methodologies have been applied to structural studies of the membrane-bound HIV-1 fusion peptide. This peptide is derived from a domain of the HIV-1 gp41 envelope protein, which is critical for viral–host cell-membrane fusion. Even in the absence of the rest of the envelope protein, the fusion peptide will fuse liposomes or erythrocytes. The solid state NMR measurements demonstrate that the center of the membrane-bound HIV-1 fusion peptide is structured, while the C-terminus is highly disordered. The structural distribution at the peptide center is lipid-dependent, with the greatest degree of structural homogeneity in a lipid environment whose composition reflects that of the target T cells. When bound to the lipid mixture, the peptide center is predominately β sheet. The β -sheet structure may be diagnostic of peptide oligomerization, which is thought to be a requirement for membrane fusion activity. Although the peptide partially disrupts bilayer orientational ordering in stacked glass-plate samples, ^2H NMR demonstrates that the bilayers remain intact in the presence of the fusion peptide and are not micellized. The retention of the bilayer phase may relate to the biological requirement that the virus should fuse with, but not destroy, the target host cell membrane. © 2001 by Elsevier Science Inc.

Keywords: HIV-1; AIDS; membrane fusion; fusion peptide; solid state NMR; NMR; chemical shift; 2D exchange; magic angle spinning

Corresponding author: D.P. Weliky, Department of Chemistry, Michigan State University, East Lansing, MI 48824, USA

E-mail address: weliky@cem.msu.edu (D.P. Weliky)

INTRODUCTION

There exists a well-developed body of techniques for solving the structures of well-structured soluble proteins; these techniques include X-ray crystallography and solution nuclear magnetic resonance (NMR) spectroscopy. Techniques for studying membrane and fibrillar proteins have lagged behind those used for soluble proteins but there has been recent progress using crystallographic, solution and solid state NMR, and electron spin resonance (ESR) techniques.^{1–4} Methods for studying partially structured proteins and proteins with multiple conformations are even less developed and represent a frontier in structural biology. In this study, we discuss the progress and potential of solid state NMR spectroscopy to address problems in membrane and partially structured proteins.

The appearance and information content of liquid and solid state NMR spectra are often quite different. In liquid state NMR, orientation-dependent interactions are averaged out by molecular tumbling and a sharp (~ 10 Hz) line is observed for each protein nucleus. In contrast, in static solid state NMR samples, orientation-dependent interactions are not averaged out and are apparent through observation of a distribution (~ 100 Hz – 1 MHz) of NMR frequencies for each protein nucleus. This distribution reflects the distribution of bond orientations relative to the magnetic field for that particular nucleus type. Sharper lines can be achieved in the solid state through mechanical ‘magic angle spinning’ (MAS),⁵ but the resultant linewidths are typically still at least ten times broader than their liquid state counterparts. As will be demonstrated, the residual MAS lineshape is diagnostic of the structural homogeneity in the vicinity of the nucleus. Another means of achieving sharp lines in the solid state is through formation of macroscopically oriented samples. This works particularly well for oriented

protein/membrane samples and has been used to determine both protein structure and protein orientation in the bilayer.⁶

There are several important strengths and constraints of solid state NMR as a structural technique. Because nuclei are detected, NMR has very general application and provides atomic-resolution information. Solid state NMR signals are observed independent of the solid environment, so that proteins can be studied in hydrated lipid bilayers, fibrils, precipitates, or crystals. Additionally, solid state NMR is typically quantitative, with all nuclei of a particular type (e.g., ¹³C) contributing equally to the spectrum. The most significant constraint is low sensitivity. Typically 0.5 μmol of material is required at concentrations of ~1 mM. These amounts are comparable to those required for crystallographic or solution NMR analysis. However, unlike these other techniques, existing solid state NMR methodologies are typically not capable of providing a full protein structure. Solid state NMR techniques rely on specific ¹³C, ¹⁵N, or ²H isotopic labeling and provide information about local structure or motion in the vicinity of the labeled nuclei. Our studies have focused on local structural questions for a membrane-bound peptide derived from the N-terminus of the HIV-1 gp41 envelope protein. In the protein, this region is known as the 'fusion peptide' because of its importance in inducing membrane fusion between the virus and target cells. Insertion of the fusion peptide into the target membrane is believed to be a key step in fusion. Fusion peptides are also found in the envelope proteins of other viruses, including influenza, ebola, and measles.⁷⁻⁹

Even in the absence of the rest of the envelope protein, the HIV-1 fusion peptide binds strongly to membranes and induces fusion between liposomes or erythrocytes. Significantly, parallel mutation/fusion activity studies on the fusion peptide domain of the intact envelope protein and the free fusion peptide have shown strong correlations between viral-host cell fusion and peptide-liposome fusion.^{10,11} These results are highly suggestive that there are important similarities between the mechanism of liposome fusion induced by the fusion peptide and viral-host cell fusion induced by envelope proteins. Thus, studies on the fusion peptide should provide insight into intact viral-host cell fusion. Because specific isotopic labeling is required for solid state NMR studies, and is done more straightforwardly on peptides than intact envelope proteins, our current studies focus on the isolated peptide. Future studies will employ biological expression of larger envelope protein domains, which include the fusion peptide.

The fusion peptide is typically considered to be about the first twenty residues of gp41. This is a fairly conserved domain with a 23-residue FP23 consensus sequence H-Ala-Val-Gly-Ile-Gly-Ala-Leu-Phe-Leu-Gly-Phe-Leu-Gly-Ala-Ala-Gly-Ser-Thr-Met-Gly-Ala-Arg-Ser-NH₂. The presence of six glycines suggests some conformational flexibility, which may be related to its fusogenicity. In particular, envelope protein-mediated fusion decreases by at least twentyfold with point mutation to valine of either of the two glycines in the highly conserved FLGFLG motif in the peptide center.^{12,13} Structural studies on the membrane-bound fusion peptide by techniques such as circular dichroism, infrared, and ESR provide a complex structural picture that suggests a distribution of secondary structures and membrane orientations, as well as possible oligomerization.¹⁰

METHODOLOGY

Peptide Synthesis

The 23-residue fusion peptide FP23 was synthesized using standard HOBt/HBTU/FMOC chemistry on an ABI 431A synthesizer. Typical coupling time was 2 h. The syntheses incorporated ¹³C carbonyl labeled amino acids, which were FMOC-derivatized by standard protocols.^{14,15} In addition, an epitope peptide HGRVGIYFGMK from tryptophan synthase was synthesized by standard methods.¹⁶

Preparation of Membrane-Bound Fusion Peptide Samples for MAS Measurements

Most samples were made by mixing freshly prepared peptide solutions with lipid dispersions or lipid vesicles at the desired peptide:lipid ratio. The peptide concentrations were typically 10–150 μM in 4 or 30 ml of 5 mM HEPES, pH 7, and the peptide:lipid mole ratios were typically 1:20–1:200.

In general, two classes of lipid were used. Initially, samples were made with di-O-tetradecylphosphatidylcholine (DTPC), a neutral saturated 14-carbon chain ether-linked lipid, which is 'NMR-friendly' because it doesn't have any carbonyl carbons and hence doesn't contribute any natural abundance NMR signal in the carbonyl region. For most later experiments, samples were made using a mixture reflecting the approximate lipid and cholesterol content of target T-cells.¹⁷ This mixture is denoted as LM and contained the synthetic lipids 1-palmitoyl-2-oleoyl-sn-glycero-3-phosphocholine (POPC), 1-palmitoyl-2-oleoyl-sn-glycero-3-phosphoethanolamine (POPE), 1-palmitoyl-2-oleoyl-sn-glycero-3-[phospho-L-serine] (POPS), sphingomyelin, phosphatidylinositol (PI), and cholesterol in a 0.33:0.17:0.07:0.07:0.03:0.33 mole ratio.

The peptide:lipid mixtures were kept at room temperature overnight to ensure maximum peptide:lipid binding. Subsequent centrifugation of the peptide-lipid complex, typically at 100,000 – 150,000 × g for 2–4 h, pelleted down the complex and left unbound peptide in the supernatant. Peptide/lipid binding was determined by measuring the peptide concentration in the solution before adding lipid and after centrifugation (by the BCA assay). Controls were run with peptide-only samples to ensure that the peptide did not pellet by itself.

In some earlier experiments, samples were made by mixing the peptide and lipid in 200 μl total volume. To measure peptide binding in these samples, additional water (~800 μl) was added, the samples were vortexed and then centrifuged, and the peptide concentration was measured in the supernatant. The peptide binding was typically nearly quantitative in these samples.

Preparation of Oriented Membrane Samples

Samples were typically made by placing lipid dispersions containing bound fusion peptide on glass plates, allowing bulk water to evaporate, stacking the plates and placing them in a square glass tube, and incubating at 40°C and 90% humidity for a few days. The tube was then epoxy-sealed with a Kel-F plug.

MAS Solid State NMR Measurements

1D Spectra were obtained on a 400-MHz Varian VXR spectrometer using a double resonance magic angle spinning (MAS) probe. The detection channel was tuned to ^{13}C and the decoupling channel was tuned to ^1H . 800 μs of 45-kHz cross-polarization and 70-kHz ^1H decoupling were used. Increased decoupling had no effect on the observed linewidths. Strong signals could not be observed above -20°C , presumably because of signal attenuation by motion. For this reason, spectra were taken at -50°C and two approaches were taken to cooling the samples. In the first method, the samples were slowly cooled in the NMR probe while slowly spinning them. In the second method, the samples were quick-frozen by immersing the sample rotors in liquid nitrogen. The spectra did not depend on the rate with which the samples were cooled nor on freeze/thaw cycling.

2D MAS exchange experiments were made on membrane-bound fusion peptide that was ^{13}C carbonyl labeled at Leu-7 and Phe-8 (FP23-L7F8). The rotor-synchronized NMR pulse sequence was $(\text{CP}) - t_1 - (\pi/2) - \tau - (\pi/2) - t_2$, where (CP) represents cross-polarization, t_1 is the evolution period, τ is the exchange period, and t_2 is the detection period.^{18–20} 2D MAS exchange is a method to determine the dihedral angles (ϕ, ψ) that define the secondary structure at the more C-terminal labeled residue, in this case Phe-8. Spectra were taken at 2.5 kHz spinning speed and secondary structure was calculated by comparing experimental off-diagonal crosspeak intensities with intensities calculated for different pairs of (ϕ, ψ) dihedral angles. 1 ppm and 2 ppm of line broadening was used for the F2 and F1 dimensions, respectively, and individual integrated peak intensities were calculated from points within 0.75 ppm of the peak. In the 2D analysis, the total squared deviation $\chi^2(\phi, \varphi)$ between experiment and simulation was evaluated as:

$$\chi^2(\phi, \varphi) = \sum_i [E_i - \lambda(\phi, \varphi)S_i(\phi, \varphi)]^2 / \sigma^2, \quad i = 1 \text{ to } N,$$

where E_i and $S_i(\phi, \varphi)$ are experimental and simulated off-diagonal crosspeak intensities, σ^2 is the mean-squared uncertainty per data point, $\lambda(\phi, \varphi)$ is a scaling factor calculated to minimize χ^2 at each ϕ and φ pair, and N is the total number of data points. The simulated crosspeak intensity pattern for a (ϕ, ψ) pair is the same as that for a $(-\phi, -\psi)$ pair so that the data cannot distinguish between each member of the pair. Measurements on the polycrystalline tripeptide Ala-Gly-Gly and the membrane-bound helical peptide melittin gave an estimated uncertainty of $\sim \pm 20^\circ$ in dihedral angle determination by this method.

Oriented Sample NMR Measurements

Bloch decay ^{31}P spectra were taken on a homebuilt static double resonance probe using 45-kHz ^1H decoupling. ^{13}C CP spectra were taken on the same probe with 45-kHz CP and with 67-kHz ^1H decoupling.

^2H Solid State NMR Measurements on Fusion Peptide/Lipid Dispersions

Samples were prepared containing LM dispersion with bound peptide. In the lipid mixture, POPC was replaced with dimyristoylphosphatidylcholine (DMPC) that was deuterated along its acyl sidechains. Spectra were taken on a single resonance

wideline probe using a solid echo sequence $(\pi/2) - \tau - (\pi/2) - \tau$ with a 7 μs $\pi/2$ pulse length and 30 μs τ interval.

RESULTS

1D Solid State NMR MAS Measurements on the Membrane-Bound Fusion Peptide

Figure 1 displays the MAS solid state NMR spectra of the isotropic carbonyl region of different ^{13}C carbonyl labeled peptides. The large differences between the observed linewidths can be correlated with the degree of local structural order in the peptide. Figure 1 a, b displays the two extrema of a crystalline peptide with 1-ppm linewidths and a random coil epitope peptide in frozen solution with 6-ppm linewidth.

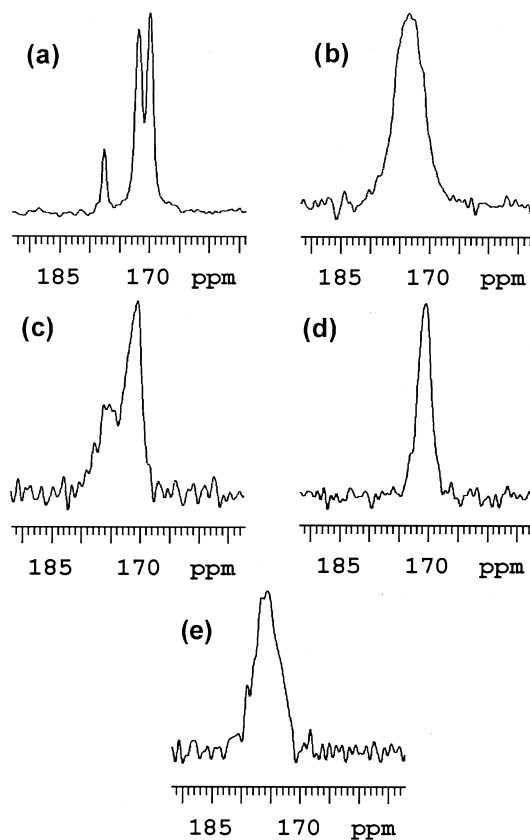


Figure 1. 1D CP/MAS solid state NMR spectra of the isotropic carbonyl region of peptides. (a) Polycrystalline Ala-Gly-Gly. 5% of the molecules are doubly ^{13}C carbonyl labeled at Ala-1 and Gly-2. (b) Epitope peptide HGRVGIY-FGMK from tryptophan synthase at 20 mM concentration in frozen solution. The peptide has a ^{13}C carbonyl label at Phe-8. (c) DTPC-bound FP23-F8 fusion peptide. (d) LM-bound FP23-F8 fusion peptide. (e) LM-bound FP23-A21 fusion peptide. Spectra (b)–(e) were taken at -50°C with 12–24 h of signal averaging and a 0.5 s recycle delay. Spectra (c)–(e) are difference spectra between labeled and unlabeled membrane-bound peptide samples with each sample containing 0.5 μmol peptide. Spectra (c) and (d) are at a 1:200 peptide:lipid mole ratio; and spectrum (e) is at a 1:80 peptide:lipid mole ratio.

Figure 1c and Figure 1d display the respective spectra for DTPC-bound and LM-bound FP23-F8 (FP23 with a single F8 ^{13}C carbonyl backbone label). Each of these spectra is actually a difference spectrum between a spectrum of the membrane-bound Phe-8 carbonyl labeled peptide and the spectrum of the membrane-bound unlabeled peptide. Difference spectroscopy is necessary because of spectral overlap between the labeled Phe-8 nucleus and natural abundance signals from lipid carbonyls and/or from unlabeled carbonyls in the peptide. The displayed difference spectra only contain contributions from the labeled Phe-8.

In Figure 1d, the ~ 2.5 -ppm full-width at half-maximum (FWHM) linewidth for the Phe-8 carbonyl demonstrates that this region of the LM-bound peptide is fairly well-structured, although not crystalline. The symmetric lineshape suggests a relatively narrow distribution of structures around a most probable structure. In contrast, the DTPC-bound peptide lineshape has at least two components, one of which is centered at the chemical shift of the LM-bound line profile and another of which is broader and to higher ppm of the LM line profile. These two components likely represent distinct populations of peptides with different local structural distributions in the vicinity of Phe-8. These data demonstrate that fusion peptide structural populations are lipid-dependent. Although the precise lipid compositional factor(s) that cause the difference are not understood, the spectra to date indicate that these differences are not due to the presence of cholesterol or phosphatidylinositol in the LM samples and their absence in the DTPC samples. For the DTPC samples, the spectra do depend somewhat on the peptide:lipid ratio. At a peptide:lipid ratio of 1:20, the broad downfield component is highly attenuated relative to the upfield component and the spectrum looks similar to Figure 1d. Figure 1e displays the difference spectrum of LM-bound FP23-A21, i.e., FP23 which is ^{13}C carbonyl labeled at Ala-21. The linewidth is ~ 5 ppm, which is twice that of FP23-F8 and close to that of an unstructured peptide. These data indicate that the membrane-bound peptide is substantially more disordered at its C-terminus than at its center.

NMR Structural Measurements

The observed peak carbonyl chemical shift of 171 ppm for LM-bound FP23-F8 is consistent with a nonhelical conformation.²¹ Further conformational measurements were made using 2D exchange spectroscopy on a DTPC-bound FP23-L7F8 sample whose 1D spectrum was predominately composed of a line with a 171-ppm peak chemical shift and 2-ppm FWHM linewidth. The experimental 2D spectrum and secondary structure fit are displayed in Figure 2a and Figure 2b, respectively. The best fit for the off-diagonal crosspeak intensity pattern is given by the smallest χ^2 (the darkest region) at $(-135^\circ, 130^\circ)$. The shaded contours are separated by two units of χ^2 , which corresponds to about one standard deviation in (ϕ, ψ) . The data are also consistent with $(135^\circ, -130^\circ)$ best-fit angles but these are sterically highly unlikely.²² The best-fit secondary structure from 2D MAS exchange is close to that of an ideal antiparallel β sheet and is consistent with the observed nonhelical chemical shift.

Peptide Effects on Membranes

Figure 3 displays the effect of the peptide on bilayer orientation in glass-plate-oriented samples at 30°C. In the ab-

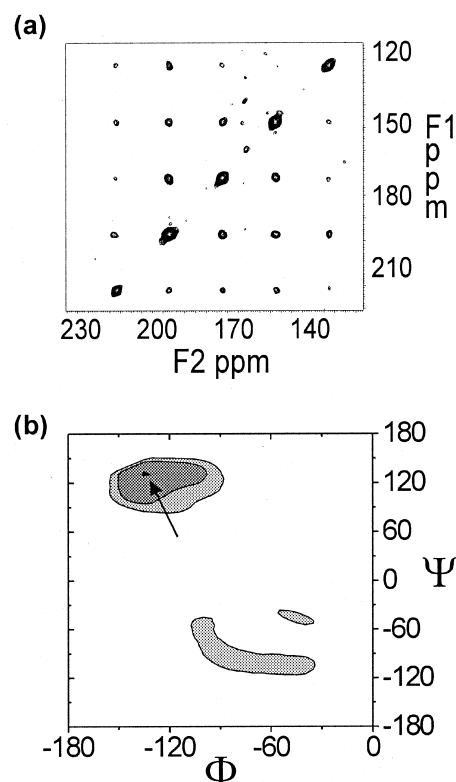


Figure 2. (a) Rotor-synchronized 2D MAS exchange spectrum; and (b) secondary structure analysis of 2 μmol FP23-L7F8 bound to DTPC. The peptide:lipid mole ratio was 1:20 and the sample included 50 mM phosphate buffer. The magic angle spinning speed was 2.5 kHz, the exchange time τ was 500 msec, the recycle delay was 0.5 s, and 72 t_1 points were taken with a t_1 increment of 40 μs . The data represent five days of signal averaging. In (b), a plot is shown for the mean square deviation χ^2 (normalized to spectral noise) between the experimental off-diagonal crosspeak intensities and calculated crosspeak intensities for a grid of F8 dihedral angles. The best-fit conformation is marked with an arrow at $\phi = -135^\circ$, $\psi = 130^\circ$. The shading levels represent: black, $\chi^2 < 6.5$; dark grey, $6.5 < \chi^2 < 8.5$; light grey, $8.5 < \chi^2 < 10.5$; white, $\chi^2 > 10.5$.

sence of peptide, strong orientational ordering is demonstrated by the variation in ^{31}P (Figure 3a, Figure 3c) and ^{13}C (Figure 3b, Figure 3d) chemical shifts as a function of sample orientation in the magnetic field. The spectra in Figure 3a and Figure 3b were taken with the glass-plate normal parallel to the external magnetic field, while those in Figure 3c and Figure 3d were taken with the normal perpendicular to the external magnetic field. The ^{31}P spectra probe the orientational order of the lipid headgroups and the ^{13}C spectra probe the orientational order of the lipid acyl sidechains. Figure 3e–3h displays similar spectra for a sample containing 5 mole percent FP23. Bilayer orientation is still demonstrated through a variation in peak chemical shift but the broader lines are diagnostic of greater orientational disorder. One possible explanation for this observation is that FP23 disrupts the bilayer physical phase, perhaps

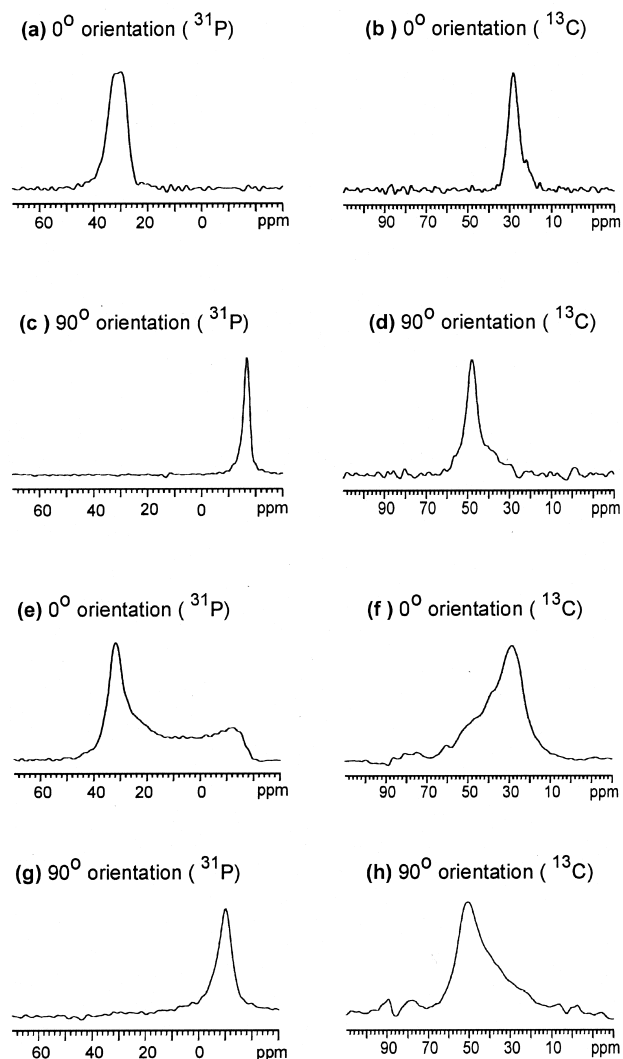


Figure 3. 30°C solid state NMR spectra of oriented LM lipids in the absence (a–d) and presence (e–h) of fusion peptide. The LM lipids are oriented between stacked glass plates and the marked orientation refers to the angle between the glass-plate normal and external magnetic field direction. The ^{31}P spectra probe the orientational ordering of the lipid headgroups and the ^{13}C spectra probe the orientational ordering of the lipid sidechains. Uniform lipid orientational ordering is observed in the absence of peptide and partial ordering is observed in the presence of peptide.

through partial micellization. However, ^2H NMR measurements displayed in Figure 4a–4d demonstrate that this possibility is unlikely.²³ These data show only minor changes in the lipid sidechain ^2H spectra for lipid dispersions in the presence of FP23. For comparison, Figure 4e–4f shows that the LM ^2H spectra are highly modified in the presence of the hemolytic bee venom peptide melittin. At high melittin concentrations, the presence of a sharp isotropic line is a marker of rapid isotropic lipid motion and micellization, as has been also observed by other investigators.²⁴

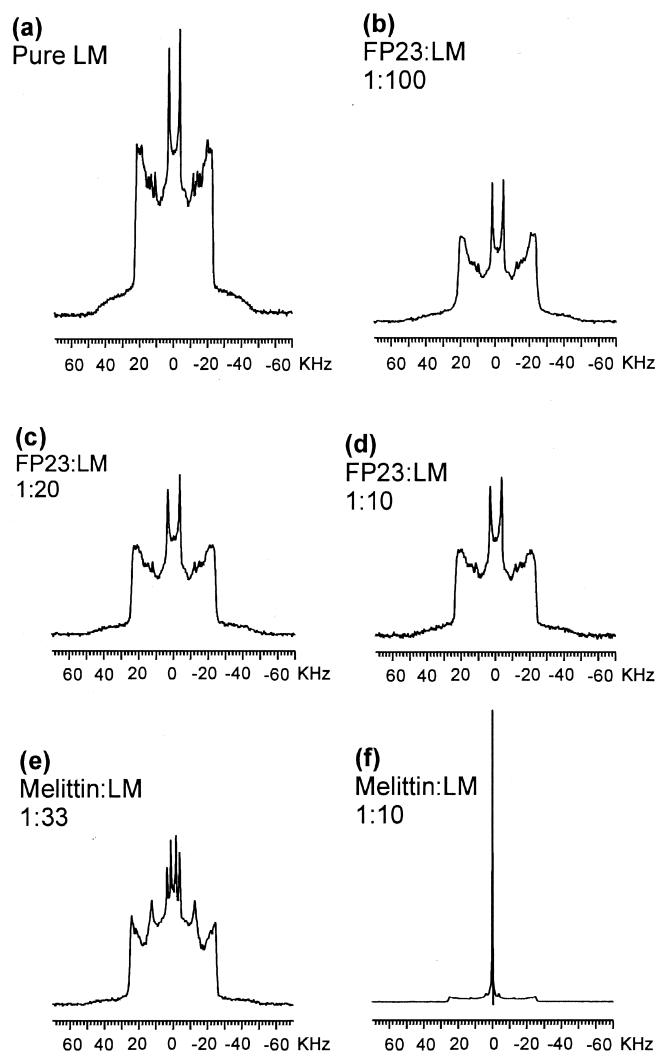


Figure 4. Solid state ^2H NMR spectra of unoriented static LM lipid dispersions at 35 °C: (a) in the absence of any peptide; (b)–(d) with bound FP23; and (e),(f) with bound melittin. The LM contains ^2H acyl sidechain-labeled DMPC. FP23 has minor effect on the ^2H spectra, while melittin induces a large increase in isotropic motion.

DISCUSSION

As observed in Figure 1, the solid state NMR lineshape of a single carbonyl nucleus provides a means of assessing the structural order in the vicinity of that nucleus. This type of information content from solid state NMR is very different from that for solution NMR in which only an average chemical shift is observed. The solid state NMR approach to assessing local structural order is quite general because of the wide availability and relative low expense of most carbonyl labeled amino acids. Although all of the results presented here apply for selectively labeled peptides, the same basic approach should work for intact proteins for which the selective labeling is biosynthetic.

The differing lineshapes in Figure 1c and Figure 1d demonstrate that the fusion peptide structural distributions at the Phe-8 residue are lipid-dependent. The peptide central region is

more structured in its interaction with the T-cell lipid composition than with the single DTPC lipid type. Interestingly, Figure 1c demonstrates that peptides bind to pure DTPC with distinct structural distributions, each of which has significant population. The lower ppm distribution is likely similar to that for the LM-bound peptide while the other corresponds to a different set of conformations. In addition, the broad linewidth in Figure 1e shows that the C-terminus of the peptide is nearly random coil.

As displayed in Figure 1 and Figure 2, measurements of solid state NMR chemical shifts and 2D exchange spectra can be used to determine the most probable secondary structure for a particular residue in a noncrystalline membrane-bound peptide. For the Phe-8 residue, the most probable structures for the 171-ppm distribution are β sheet. There is a strong possibility that this β -sheet structure is diagnostic of oligomer formation in the membrane by the fusion peptide. This finding may have biological significance because formation of fusion peptide oligomers has been linked to fusion activity for both envelope protein-mediated fusion and for liposome fusion mediated by fusion peptides.^{11,25} The structures of possible membrane-bound fusion peptide oligomers will be investigated in future solid state NMR measurements of interpeptide distances. In cases such as that shown in Figure 1c for which two or more conformational distributions are resolved near a particular nucleus, it should be possible to use solid state NMR techniques such as 2D exchange to determine the most probable conformation in each distribution. In principal, even in the case of broad lines, the structures associated with different regions of the lineshape could be assessed by separate analyses of these regions. Alternatively, one could analyze the entire lineshape using a model based on a structural distribution.²⁶ A potential difficulty in quantitative solid state NMR analyses of broad structural distributions is the lack of good model systems to test whether the solid state NMR approach gives correct results. In the case of a broad line such as Figure 1b, molecular dynamics calculations could be used to predict the distribution of conformations, followed by quantum mechanical calculations to predict the distribution of chemical shifts associated with the conformational distribution. This sort of approach should enable researchers to show whether a particular distribution is consistent or inconsistent with the experimental lineshape and with data from 2D exchange or other solid state NMR structural refinement techniques.

Figure 3 and Figure 4 demonstrate how solid state NMR can also be used to understand the effect of fusion peptides on membranes. Figure 3 shows that the fusion peptide partially disrupts bilayer order in glass-plate samples, while Figure 4 reveals that it does not induce a large change in the overall motion and structure of the bilayer. This is in large contrast to the hemolytic bee venom peptide melittin, which micellizes the bilayer. These differing data may be related to the different functions of the two peptides. In particular, viral infection relies on fusion but not destruction of lipid bilayers. Future studies will investigate more subtle interaction of the fusion peptide with membranes through its effect on lipid nuclei relaxation times. In addition, the glass-plate samples will be used to probe the orientational distribution of the fusion peptide in the bilayer.

CONCLUSIONS

The solid state NMR lineshape of a protein backbone carbonyl nucleus is a general diagnostic of the local conformational distribution in the vicinity of that nucleus. Measurements of carbonyl chemical shift and 2D exchange spectra provide information about the most probable conformation in this distribution. Application of such solid state NMR methodologies to the membrane-bound HIV-1 fusion peptide demonstrates that the peptide center is structured, although not crystalline, while the C-terminus is highly disordered. The structural distribution at the peptide center is lipid-dependent with the greatest degree of structural homogeneity in a lipid environment whose composition reflects that of target T cells. When bound to the lipid mixture, the peptide center is predominately β sheet. Although the peptide partially disrupts bilayer orientation in stacked glass-plate samples, ²H NMR demonstrates that the bilayers remain intact in the presence of the fusion peptide and are not micellized.

ACKNOWLEDGMENTS

D.P.W. acknowledges support from Michigan State University and from a Camille and Henry Dreyfus Foundation New Faculty Award.

REFERENCES

- 1 Palczewski, K., Kumasaka, T., Hori, T., Behnke, C.A., Motoshima, H., Fox, B.A., Le Trong, I., Teller, D.C., Okada, T., Stenkamp, R.E., Yamamoto, M., and Miyano, M. Crystal structure of rhodopsin: A G protein-coupled receptor. *Science* 2000, **289**, 739–745.
- 2 MacKenzie, K.R., Prestegard, J.H., and Engelman, D.M. A transmembrane helix dimer: structure and implications. *Science* 1997, **276**, 131–133
- 3 Benzinger, T.L., Gregory, D.M., Burkoth, T.S., Miller-Auer, H., Lynn, D.G., Botto, R.E., and Meredith, S.C. Propagating structure of Alzheimer's beta-amyloid(10–35) is parallel beta-sheet with residues in exact register. *Proc. Natl. Acad. Sci. U. S. A.* 1998, **95**, 13407–13412
- 4 Farrens, D.L., Altenbach, C., Yang, K., Hubbell, W.L., and Khorana, H.G. Requirement of rigid-body motion of transmembrane helices for light activation of rhodopsin. *Science* 1996, **274**, 768–770
- 5 Schmidt-Rohr, K., and Spiess, H.W. *Multidimensional Solid-State NMR and Polymers*. Academic Press, San Diego, 1994
- 6 Cross, T.A., and Opella, S.J. Solid-state nmr structural studies of peptides and proteins in membranes. *Curr. Opin. Struct. Biol.* 1994, **4**, 574–581
- 7 Hernandez, L.D., Hoffman, L.R., Wolfsberg, T.G., and White, J.M. Virus–cell and cell–cell fusion. *Annu. Rev. Cell. Dev. Biol.* 1996, **12**, 627–661
- 8 Blumenthal, R., and Dimitrov, D.S. Membrane fusion. In *Handbook of Physiology, Section 14: Cell Physiology*, Hoffman, J.F., and Jamieson, J.C., Eds., Oxford, New York, 1997, pp. 563–603
- 9 Jahn, R., and Sudhof, T.C. Membrane fusion and exocytosis. *Ann. Rev. Biochem.* 1999, **68**, 863–911
- 10 Durell, S.R., Martin, I., Ruyschaert, J.M., Shai, Y., and Blumenthal, R. What studies of fusion peptides tell us

- about viral envelope glycoprotein-mediated membrane fusion (review). *Mol. Membr. Biol.* 1997, **14**, 97–112
- 11 Kliger, Y., Aharoni, A., Rapaport, D., Jones, P., Blumenthal, R., and Shai, Y. Fusion peptides derived from the HIV type 1 glycoprotein 41 associate within phospholipid membranes and inhibit cell–cell fusion. Structure–function study. *J. Biol. Chem.* 1997, **272**, 13496–13505
 - 12 Delahunty, M.D., Rhee, I., Freed, E.O., and Bonifacino, J.S. Mutational analysis of the fusion peptide of the human immunodeficiency virus type 1: Identification of critical glycine residues. *Virology* 1996, **218**, 94–102
 - 13 Myers, G., et al., Eds. *Human Retroviruses and AIDS* 1988, 1989, 88
 - 14 Chang, C.D., Waki, M., Ahmad, M., Meienhofer, J., Lundell, E.O., and Haug, J.D. Preparation and properties of N-Alpha-9-Fluorenylmethoxycarbonylamino acids bearing Tert-Butyl Side-Chain protection. *Intl. J. Peptide Protein Res.* 1980, **15**, 59–66
 - 15 Lapatsanis, L., Milias, G., Froussios, K., and Kolovos, M. Synthesis of N-2,2,2-(Trichloroethoxycarbonyl)-L-amino acids and N-(9-Fluorenylmethoxycarbonyl)-L-amino acids involving succinimidoxo anion as a leaving group in amino-acid protection. *Synthesis-Stuttgart* 1983, 671–673
 - 16 Guijarro, J.I., Djavadi-Ohanian, L., Baleux, F., Delépierre, M., and Goldberg, M.E. Does a peptide bound to a monoclonal antibody always adopt a unique conformation? *Res. Immunol.* 1998, **149**, 127–137
 - 17 Aloia, R.C., Tian, H., and Jensen, F.C. Lipid composition and fluidity of the human immunodeficiency virus envelope and host cell plasma membranes. *Proc. Natl. Acad. Sci. U.S.A.* 1993, **90**, 5181–5185
 - 18 Luz, Z., Spiess, H.W., and Titman, J.J. Rotor synchronized Mas 2-dimensional exchange NMR in solids – principles and applications. *Israel J. Chem.* 1992, **32**, 145–160
 - 19 Weliky, D.P., and Tycko, R. Determination of peptide conformations by two-dimensional magic angle spinning NMR exchange spectroscopy with rotor synchronization. *J. Am. Chem. Soc.* 1996, **118**, 8487–8488
 - 20 Tycko, R., Weliky, D.P., and Berger, A.E. Investigation of molecular structure in solids by two-dimensional NMR exchange spectroscopy with magic angle spinning. *J. Chem. Phys.* 1996, **105**, 7915–7930
 - 21 Wishart, D.S., Sykes, B.D., and Richards, F.M. Relationship between nuclear magnetic resonance chemical shift and protein secondary structure. *J. Mol. Biol.* 1991, **222**, 311–33
 - 22 Cantor, C.R., and Shimmel, P.R. *Biophysical Chemistry*. W.H. Freeman, New York, 1980
 - 23 Bloom, M., Evans, E., and Mouritsen, O.G. Physical properties of the fluid lipid-bilayer component of cell membranes: a perspective. *Q Rev Biophys* 1991, **24**, 293–397
 - 24 Dempsey, C.E. The actions of melittin on membranes. *Biochim. Biophys. Acta.* 1990, **1031**, 143–161
 - 25 Freed, E.O., Delwart, E.L., Buchschacher, G.L., Jr., and Panganiban, A.T. A mutation in the human immunodeficiency virus type 1 transmembrane glycoprotein gp41 dominantly interferes with fusion and infectivity. *Proc. Natl. Acad. Sci. U. S. A.* 1992, **89**, 70–74
 - 26 Long, H.W. and Tycko, R. Biopolymer conformational distributions from solid-state NMR: α -helix and 3_{10} -helix contents of a helical peptide. *J. Amer. Chem. Soc.* 1998, **120**, 7039–7048